Half-lives of cluster radioactivity within a model including superfluid phenomena and resonance effects

I. Silisteanu
Department of Theoretical Physics, Institute of Atomic Physics, Bucharest MG-6, Romania

W. Scheid
Institut für Theoretische Physik der Justus-Liebig-Universität, D-35392 Giessen, Germany
(Received 1 July 1994; revised manuscript received 5 December 1994)

A model is proposed for studying exotic cluster radioactivities. This model is general and realistic that one can test the actual main treatments of clustering and penetration phenomena in nuclear many-particle systems. A reliable and rather simple approximation derived in this model is found on the continuum hopping treatment of clustering and on an integral formalism of decay dynamics including resonance scattering effects. The half-life estimates are performed for experimentally detected cluster radioactivities and for the most interesting cases under the current experimental search.

PACS number(s): 21.60.Gx, 23.70.+j, 21.10.Tg

I. INTRODUCTION

During recent years, the cluster radioactivity (CR) phenomenon has been intensively studied both theoretically and experimentally. The pioneering work of Refs. [1,2] has opened a new interesting field in low-energy physics with many exciting possibilities. Continuing refinements of the theory and computing techniques have brought considerable advances. It is now possible to explain the effects of the "fine structure" [3,4] and excited states [5] in close relation with single-particle and collective excitations, multiple resonances formed in collective excitations [6,7], and even soliton excitations at the nuclear surface [8]. The results are interesting for two reasons. On the one hand, they give new life to the old problem of nuclear stability with respect to α decay and fission; on the other hand, they suggest that CR may be due to the onset of static and dynamic instabilities.

The theories are based on (i) models for the nuclear Hamiltonian that generate bound, resonance, and cluster states; (ii) methods to treat the tunneling in many-particle systems, namely, the dynamics in the classically forbidden region.

In this work we propose an unified model for the cluster degrees of freedom in nuclei. The model is constructed as follows. Using a simple description of the nuclear structure we construct the decay amplitudes of resonances states into free channel states. At this point we apply the continuum hopping model (CHM) to construct the cluster formation amplitude (CFA) in the harmonic-oscillator basis with a Gaussian probability distribution.

The tunneling process is described with the integral formalism (IF) [6,7] derived within the Feshbach theory of nuclear reactions. The resulting approach reduces the calculation of decay rates to the problem of finding the eigenvalues of a collective Hamiltonian. Furthermore, the model including the CHM amplitude and pairing residual interaction shows signatures of superfluid effects in the clustering and resonance effects in the fragment scattering.

This paper is organized as follows. We review the basic formalisms necessary for the calculation of decay rates in Sec. II. The methods for obtaining the cluster formation probabilities are discussed in Sec. III. The connection of the basic formalism with the model cluster amplitudes is the object of Sec. IV. Details of the used computing methods are given in Sec. V. Results and conclusions are summarized in Secs. VI and VII.

II. INTEGRAL FORMALISM

The microscopic approach of cluster decay phenomena starts from a mean field or from mean field wave functions of the many-particle system. The system is described with Slater determinants associated with absolute and relative minima of the energy corresponding to the equilibrium shape of a nucleus. The wave functions are modified in the barrier-penetration process by the residual interaction which then provides the dynamics of tunneling. In order to be applicable and physically interesting, the wave functions should describe the interplay between the nuclear structure and reaction mechanism. In this section we review the essentials of reducing the many-particle Hamiltonian to a "one-body" Hamiltonian. This new Hamiltonian provides a reliable model description for clustering and tunneling. The first problem is to separate the structure part from the part describing the decay dynamics. The microscopic description [6,7] of the decay process needs a complete set of basic states, namely, the bound states $|\Psi_k\rangle$ of the system and scattering states $|\chi_E^c\rangle$ describing the relative motion in channel c. The states $|\Psi_k\rangle$ may be obtained by diagonalizing a model Hamiltonian and then the scattering states are obtained by solving the integral equation

$$(H-E)\mid\chi^c_E\rangle=\sum_k\langle\Psi_k\mid H\mid\chi^c_E\rangle\mid\Psi_k\rangle\ , \tag{1}$$

where H is the Hamiltonian of the system, E is the energy, c is the channel index, and k denotes a set of discrete quantum numbers. We consider here a system of A particles that can decay into a two-body channel c with fragments having A_1 and A_2 nucleons. For a system of interacting nucleons the Hamiltonian of the system is decomposed as

$$H=H_1+H_2+T(r)+V(r)=H_1+H_2+H_{\rm coll}\ , \tag{2}$$

where H_i $(i=1,2)$ are the internal Hamiltonians of the fragments and the collective part includes the kinetic and potential energies.

The width associated with the decay of state k into the channels c is given by [6, 7, 13]

$$\begin{aligned}\Gamma_k&=2\pi\sum_c\mid\langle\Psi_k\mid H\mid\chi^c_E\rangle\mid^2\\&=2\pi\sum_c\left|\langle\Psi_k\mid\chi^c_{E,0}\rangle/\langle\Psi_k\mid\chi^c_{E,k}\rangle\right|^2=\sum_c\Gamma_{c,k}\ ,\end{aligned} \tag{3}$$

where $\mid\chi^c_{E,k(0)}\rangle$ are solutions of the system of equations $(H-E)\mid\chi^c_{E,k}\rangle=\mid\Psi_k\rangle$ and $(H-E)\mid\chi^c_{E,0}\rangle=0$.

The partial width Γ_{ck} can be obtained by using a model Hamiltonian for the scattering states. First, by integrating over the internal coordinates of the fragments and also angular coodinates of relative motion, we extract in Eq. (3) the cluster formation amplitude (CFA)

$$I_{ck}(r)=r\langle\Psi_k\mid\mathcal{A}\{[\Phi_1(\eta_1)\Phi_2(\eta_2)Y_{lm}(\hat r)]_c\}\rangle \tag{4}$$

as an antisymmetrized projection of the parent wave function on the channel wave function $\mid\Phi_c\rangle=\mid[\Phi_1(\eta_1)\Phi_2(\eta_2)Y_{lm}(\hat r)]_c\rangle$. In Eq. (4) $\mathcal{A}$ is the intercluster antisymmetrizer, $\Phi_{\rm i}$ $(i=1,2)$ are the internal wave functions of the fragments, and the $\langle\mid\rangle$ means integration over internal coordinates and angular coordinates of relative motion.

Second, the partial width is obtained by integrating over the radial distance (collective variable):

$$\Gamma_{ck}=2\pi\left|\frac{\int_0^\infty I_{ck}(r)u^0_c(r)dr}{\int_0^\infty I_{ck}(r)u^k_c(r)dr}\right|^2\ , \tag{5}$$

where $u^{k(0)}_c$ are solutions of the system of equations

$$[T(r)+V(r)-Q]\,u^k_c(r)=I^k_c(r)\ , \tag{6}$$

$$[T(r)+V(r)-Q]\,u^0_c(r)=0\ , \tag{7}$$

describing the dynamics of the system evolving in the channel c (with the emission energy $Q=E-E_1-E_2$) at small and large separations, respectively. Note that the CFA appears as the inhomogeneous term in Eq. (6) and therefore the general solution of the system of Eqs. (6),(7) depends on CFA. Thus, in the integral formalism it is impossible to distinguish exactly between the cluster formation and barrier penetration processes. However, the formation stage may be understood as a part of the process of barrier penetration itself.

III. CONTINUUM HOPPING MODEL

In order to separate the cluster degree of freedom from the single-particle motion we define the collective Hamiltonian in Eq. (2). Applying the CHM approximation to the Hamiltonian equations (2.2) and (2.3) of Ref. [9], we represent the collective Hamiltonian by the continuous operator

$$\begin{aligned}H_{\rm coll}(r)&=-\frac{d}{dr}4\mid\lambda\mid(\kappa^2N^2-r^2)\frac{d}{dr}+(N/2-N\kappa^2M^2/2)\\&\quad+\left[\kappa^2N^3/2+(\lambda-\mid\lambda\mid)N^2/2\right]\left[1-r^2/(\kappa^2N^2)\right]+(\lambda-\mid\lambda\mid)N\\&=-\frac{d}{dr}\triangle r^2v(r)\frac{d}{dr}+E_0+V(r)+2v(r).\end{aligned} \tag{8}$$

The Hamiltonian (8) describes the collective motion of N distinguishable particles. Each of these particles is characterized by a spatial coordinate z_i as well as an internal spin coordinate. The collective coordinate r is the intercluster distance which is obtained from the collective dimensionless variable x used in Ref. [9] by transformation $r=\kappa Nx=\langle z\rangle/N$. The model parameters are κ and λ. The first parameter κ represents the strength of the two-body interaction which couples the total spatial coordinate $z=\sum_{i=1}^N z(i)$ to the expectation value of the azimuthal spin operator $M=\langle\sum_{i=1}^N\sigma_z(i)\rangle$. The second parameter λ is the strength of the residual pairing interaction which breaks the Hartree symmetry and connects only the neighboring configurations. For simplicity we only consider even N harmonic oscillators (HO) and confine the states which only include $M=\pm N$. The configuration space is truncated to the number of excitation quanta $\nu\le4$ of the shifted HO which only connects states M with $M\pm4$.

In the Hamiltonian (8) the matrix elements of the residual interaction lead to a kinetic term $T(r)=-\frac{d}{dr}4\mid\lambda\mid(\kappa^2N^2-r^2)\frac{d}{dr}$ with an inertial mass. The inertial mass is

$$D(\kappa N)^2=\hbar^2\frac{(\kappa N)^2}{8\mid\lambda\mid(\kappa^2N^2-r^2)}=-\hbar^2\frac{n^2}{2v}\ , \tag{9}$$

a result first derived for the cluster decays by Baranco, Broglia, and Bertsch [10]. Notice that the inertial mass [10] $D_x=\hbar^2\left[8\mid\lambda\mid(1-x^2)\right]^{-1}=-\hbar^2n^2/2v$ only de-

pends on the matrix element of the pairing interaction v and the reduced mass number of the system $n = A_1A_2/(A_1+A_2)$. Most interesting applications of Eq. (9) in Refs. [10, 11] are based on the constant matrix element of the pairing interaction $v = -(\triangle_p^2 + \triangle_n^2)/4G$, where the nucleon pairing gapes $\triangle_p$ and $\triangle_n$ and the pairing strength G are given by the standard superfluid model [11].

We solve the Hamiltonian (8) numerically using as a basis the states $\varphi_\nu(r)$ of the Hamiltonian without the residual interaction. The Hartree Hamiltonian is then given by a shifted oscillator Hamiltonian, and the collective wave functions are just the oscillator states centered appropriately:

$$[T(r) + V(r) - Q]\,\varphi_\nu(r) = 0\,, \tag{10}$$

where $Q = E - E_1 - E_2 - E_0$ and E_0 is the collective ground state energy [the second term in Eq. (8)].

We want to determine the matrix elements of the Hamiltonian for a number of excitation quanta $\nu \neq 0$ and for a chosen decay channel making use of phase shifts. Let δ_0 be the phase shift calculated for the potential $V(r)$ of range r_t at the emission energy $Q = \hbar^2q^2/2D$, where q is the relative momentum and, let δ be the phase shift known from experiment. As we shall see one may use the wave function $\varphi_q(r)$ for scattering by the diagonal potential $V(r)$ with the usual asymptotic normalization $\varphi_q(r) \to r^{-1}\sin(qr - l\pi/2 + \delta_0)$ to deduce the matrix elements $2v(r)$ of the potential in the set of functions $\varphi_q(r)$ as q varies. The wave function $\varphi_q(r)$ in $r \leq r_t$ will coincide with the solution $\varphi_\nu(r)$ of Eq. (10) apart from normalization. We therefore write in $r \leq r_t$

$$\varphi_q(r) = A\varphi_\nu(r)\,, \tag{11}$$

where A is a constant which depends on the diagonal potential and the boundary conditions (see Sec. V).

According to the perturbative treatment of $v(r)$ [12], we recover the result (9) in terms of phase shifts

$$\int_0^\infty \varphi_q(r)2v(r)\varphi_q(r)dr = -(\hbar^2q/D)\tan(\delta - \delta_0)\,. \tag{12}$$

The close expression for the diagonal and most important off-diagonal matrix elements of the Hamiltonian is obtained if we choose $V(r)$ as a cutoff oscillator with depth $V_{\rm os}$, shape parameter b, and range r_t, and if we use Eqs. (11) and (12):

$$\int_0^\infty \varphi_\nu(r)\,[V(r) + 2v(r)]\,\varphi_\nu(r)dr$$

$$= \int_0^{r_t} \varphi_\nu^2(r)V_{\rm os}\left[1 - r^2/b^4\right]dr$$
$$-(\hbar^2q/D)(A)^{-2}\tan(\delta - \delta_0)\,.$$

This choice is equivalent to using an energy-dependent and channel-dependent potential.

In the next section we use Eqs. (9)–(11) to treat the barrier dynamics.

IV. CONNECTION OF IF AND CHM

The rates associated with the cluster degree of freedom are described in IF by the dynamic equations for some nuclear integral characteristics which may be obtained without difficulties in the CHM. Let us proceed to derive the CFA as we discussed in Sec. II. We would like to superpose only positive energy solutions (11), the only physically interesting ones at the formation stage. We start introducing the wave functions (11) in Eq. (4) by a sharply peaked even wave function $\delta(r - r_t)$ (normalized Gaussian centered in "range" $a = r - r_t$ at the touching configuration r_t) of argument $\alpha^2 = D\omega/\hbar$

$$I_{c\nu}(r) = r\langle\Phi_c(r^{-1}\varphi_q(r)\delta(r - r_t))\mid\mathcal{A}\mid\Phi_c\rangle$$
$$= \sqrt{\pi}A(\alpha a/\sqrt{\pi})^{1/2}\exp\left[-\alpha^2a^2/2\right]\varphi_\nu(r)\,, \tag{13}$$

where we take $\langle\Phi_c \mid \mathcal{A} \mid \Phi_c\rangle = 1$. The result (13) shows that the decay in the Schrödinger picture is analogous to what happens with the Gaussian wave packets constructed by superposing plane waves, and seems satisfactory. However, there is an inconsistency in the assumption of superposition of positive energy solutions only.

Using Eq. (13) in Eq. (6), we obtain from Eq. (5)

$$\Gamma = W\Gamma_0\,, \tag{14}$$

where

$$W = (\alpha a/\sqrt{\pi})\exp(-\alpha^2a^2) \tag{15}$$

is the probability of finding the cluster in the classically allowed region, and

$$\Gamma_0 = \Gamma_{\nu c} = 2\pi\left|\frac{\int_0^\infty \varphi_\nu(r)u_c^0(r)dr}{\int_0^\infty \varphi_\nu(r)u_c^\nu(r)dr}\right|^2 \tag{16}$$

is the so-called "one-body" decay width. The functions $u_c^{\nu(0)}(r)$ in Eqs. (16) are the solutions of the system of differential equations

$$[T_c(r) + V_c(r) - Q]\,u_c^\nu(r) = A\varphi_\nu(r)\,, \tag{17}$$

$$[T_c(r) + V_c(r) - Q]\,u_c^0(r) = 0\,, \tag{18}$$

describing the dynamics of the system evolving in the channel c at small and large separation, respectively. Notice that if we chose $a = 1$ fm in Eq. (15) we obtain for the formation probability the result of Ref. [13]. The created excitation by the nucleon clustering in the first stage evolves in the latter stage according to the one-body description given by Eqs. (17) and (18). In the first stage we used the independent single-particle description which is approximately valid only in the very low energy region. On the other hand, at positive subbarrier energies the unstable nucleus exhibits the resonance structure characteristic for strongly interacting many nucleons. Our aim was to show how these apparently opposing concepts can be reconciled by means of the Feshbach resonance theory of nuclear reactions, and further, by relating the param-

eters of the scattering potential to those describing the characteristics of the resonance levels, at least implicitly. The connection of CHM to IF is illustrated in Fig. 1.

The geometry of the scattering potential in Eqs. (17) and (18) is fixed for each fragment combination by using an additional condition for the resonance scattering. This latter condition is connected with the traditional inverse scattering problem at fixed energy, based on the homogeneous Eq. (18), namely, the calculation of the resonance potential and the resonance wave functions from the phase shifts as a function of one parameter (see Sec. V). Choosing the depth of nuclear potential as a resonance parameter, we first determine u_c^0 as the resonance wave function u_c^r which fulfills the asymptotic boundary conditions for Gamow scattering states. We evaluate u_c^r in a form similar to that proposed in Refs. [14] and [15]. A most important point of the solution of Eq. (18) is the calculation of the asymptotic CFA. The result depends to some extent on the boundary conditions at distances larger than the touching configuration. Since at these distances the fragment interaction is dominated by the Coulomb term, the solution φ_ν of Eq. (10) can be substituted by $u_c^r = u_c^0$ in Eq. (17). Then we obtain from Eq. (16) a one-body decay width formula which exactly coincides with the integral decay width formulas given by Breit [14] and Feshbach [15]. In this case, it is interesting that the elastic channel solution u_c^0 (or the elastic channel CFA) appears as an inhomogeneous term in Eq. (17) which determines the "inelastic" channel solution u_c^ν. This may produce the mechanism for enhanced excitation of the resonance states when the corresponding wave functions are simultaneously resonating with their resonance states in the potential.

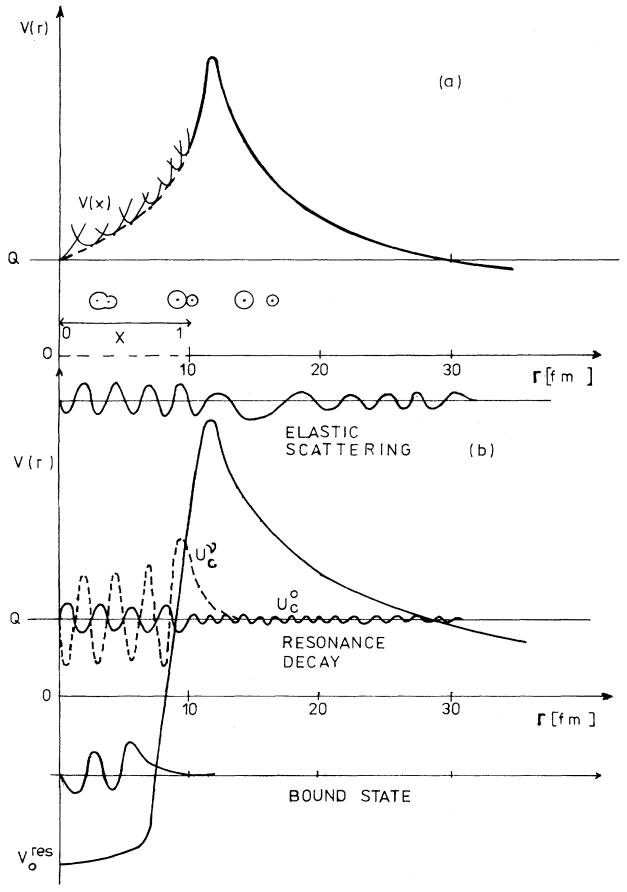

FIG. 1. (a) Schematic representation of the Hartree-Fock potential used in the continuum hopping model in Ref. [10] as a function of dimensionless deformation parameter x. At $x = 0$ the parent nucleus is assumed to be in a spherical ground state and at $x = 1$ the touching configuration of spherical fragments is shown. (b) Schematic representation of potential for clustering and resonance scattering as a function of distance between the fragments. The solution u_c^ν and u_c^0 describing the decay dynamics are compared to solutions for elastic scattering and bound states.

V. COMPUTING METHODS

A. CHM wave functions

Modeling the decay process we used three energy scales. The first is the energy of collective single-particle motion. We identify this energy with the energy of giant quadrupole vibrations which has the order of magnitude of 10–15 MeV and sets the unit scale of the oscillator frequency in Eqs. (8)–(11) and (13). The second physical energy scale is the barrier height. For spontaneous decay processes from ground states a typical value of the barrier height is 5 MeV. Thus the model Hamiltonian (8) should have [9] an effective barrier height of about $[\kappa^2 N^3/2 + (\lambda - |\lambda|)N^2/2] \simeq (1/2 - 1/3)/\hbar\omega_0$. We set the scale for λ by requiring a value [11] $v \simeq 2.8$–3.0 MeV for the matrix elements of connecting adjacent configurations. We solve Eq. (10) by a numerical diagonalization. The normalization constant A in Eq. (11) follows from the matching φ_q (and its derivative) with the free solution $\varphi_q(r) = q\,[j_l(qr)\cos(\delta_n + \delta_c) - n_l(qr)\sin(\delta_n + \delta_c)]$ at the boundary value $r = d$ (j_l and n_l are the Bessel and Neumann functions and δ_n and δ_c are nuclear and Coulomb phase shifts). For the outer region the asymptotic normalization is assumed: $\varphi_q(r) \to r^{-1}\sin(qr - l\pi/2 + \delta_n + \delta_c)$. At the resonance energy Q the wave functions φ_ν in $r < r_t$ will exactly coincide with the usual bound state wave functions of an infinite oscillator apart from normalization.

B. Fragment interaction

The potentials relevant for the decay process can be obtained assuming that (i) the mean square radius $\langle r_A^2\rangle^{1/2}$ describes the spatial size of a nucleus with A nucleons; (ii) effects due to the Pauli principle appear at distances less than $\langle r_t^2\rangle^{1/2}$ where the fragments lose their identity. The effective local potential between the two fragments, close to the mean square distance $\langle r_t^2\rangle^{1/2}$, is given by the oscillator, Coulomb, nuclear, and centrifugal terms [16]

$$V_c(r) = m\omega^2 r^2/2 - m\omega_t^2\langle r_t^2\rangle + U_c(r) + V_0 f(r, r_0, a_0) + V_{cf}(r) \ , \quad (19)$$

where m is the reduced mass of the system and ω,ω_t are the oscillator frequencies at the distances r and r_t. The Coulomb term is calculated with the fragment charge radii R_1 and R_2 and the form factor of nuclear potential f is chosen of the Woods-Saxon type with the optical model parameters [17 – 20] as input parameters. The depth of the nuclear potential V_0 is adjusted to reproduce accurately the experimental decay energy Q as an eigenenergy of the radial Schrödinger equation (18) for the elastic channel. Making the depth of nuclear potential broad or high, the scattering state $u_c^0(r)$ can be transformed into a resonance state of the discrete spectrum. This adjusted value, usually called the resonance depth, is denoted by $V_0^{\rm res}$.

C. Wave functions of relative motion

The fragment interaction contains two ingredients, a daughter-cluster potential and the requirement of orthogonality of the wave function of relative motion to Pauli forbidden states. A most important effect of the orthogonality condition is that the radial wave function of relative motion must have at least n_l nodes, where n_l is the number of forbidden states in the lth partial wave [21]. This damps the relative motion wave function in a region extending from the origin to the outermost of these required nodes, i.e., to the n_lth node. The position of the n_lth node can be accurately approximated by the outermost node of the first allowed oscillator function of the relative motion (see Fig. 2). The number of nodes is given by the Wildermuth condition

$$n_l = \sum_{i=1}^{N_c} (2n_i + l_i) \ , \quad (20)$$

where N_c is the number of nucleons of the emitted cluster and n_i, l_i are the principal and angular momentum quantum numbers of nucleons in the oscillator shell model description [6,7]. In this way it resembles qualitatively the WKB wave function with a fixed number of excitation quanta.

VI. RESULTS

The half-lives obtained in the present approximation for C, Ne, Mg, and Si cluster radioactivities are shown in Table I and also in Fig. 3 in a Geiger-Nuttall plot. In order to check the validity of the method employed, we compare our results with the available experimental data including also upper-limit estimations for decay rates (see the review of Ref. [22]). We see in Table I and Fig. 3 that the difference between our results and experimental data is within about one order of magnitude. In general, this situation is quite satisfactory with actual data, of course in the limit of accuracy of the model for ground state CR. If we compare our results with those calculated [for the same mass parameter given by Eq. (9)] within the superfluid model of Ref. [13], we observe differences. These differences may arise only due to an additional enhancement of emission caused by resonance scattering which is neglected in Ref. [13]. Also, we can see in Table I that the corrections arising from resonance scattering effects are quite important. However, the calculated lifetimes are in several cases larger than the experimental ones. Despite relatively good agreement with previous Gamow models [1,2,5,22,23] and cluster shell models [6–8,24–26],

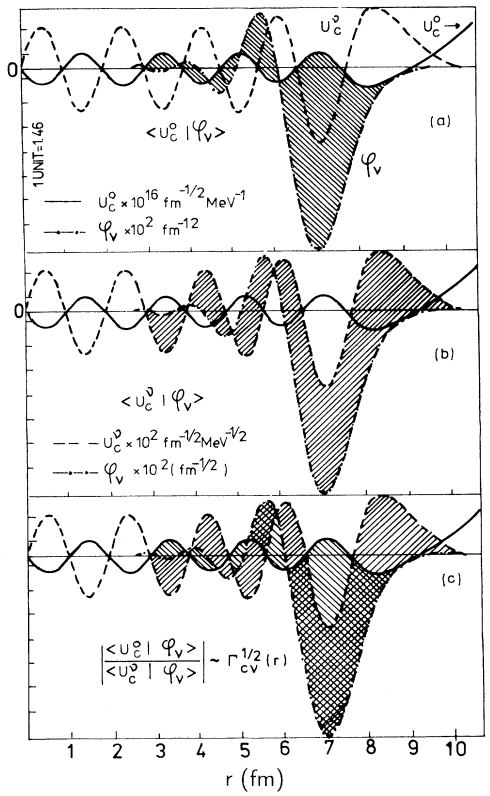

FIG. 2. (a) The cluster formation amplitude $I_{c\nu}(r)$ [$\sim \varphi_\nu(r)$] and the solutions of relative motion. $u_c^\nu(r)$, $u_c^0(r)$ given by Eq. (13) and Eqs. (17) and (18) respectively, for alpha decay of ^{210}Po (Q_α=5.304 MeV). The parameters of the scattering potential are taken from Ref. [22] (set A: V_0 = 96.44 MeV, r_0 = 1.376 fm, and a_0 = 0.625 fm^{-1}). The resonance depth $V_0^{\rm res}$ = 127.59 MeV is obtained with the procedure described in text. The number of nodes in the scattering wave function $u_c^0(r)$ is n_l = 20 and the set ($c\nu$) refers to the ground state alpha decay. The matrix element $\langle u_c^0 \mid \varphi_\nu\rangle = \int_0^r u_c^0(r)\,\varphi_\nu(r)dr$ as a function of the radial distance r between the fragment is represented by the shaded area. (b) The matrix element $\langle u_c^\nu \mid \varphi_\nu\rangle = \int_0^r u_c^\nu(r)\varphi_\nu(r)dr$ is represented by the shaded area. (c) The absolute value of the ratio of the matrix elements $\int_0^r u_c^0(r)\varphi_\nu(r)dr$ and $\int_0^r u_c^\nu(r)\varphi_\nu(r)dr$ as a function of the radial distance between the fragments. We see that the major contribution to the decay width is coming from the region of the nuclear surface (6–8 fm) marked by the double hatched area.

TABLE I. The calculated half-lives associated with cluster radioactivities in the actinide region. The decay is specified in the second column and the energy of the emitted cluster in the center-of-mass system is given in the third column. The fourth and fifth columns show the relative angular momentum and the one-body decay constant $\lambda_0=\Gamma_0/\hbar$. The present results are displayed in the sixth column. The seventh column lists the results of Ref. [13] and the last column shows the experimental half-lives taken from the review of Ref. [22].

	Initial nucleus	Emitted cluster	$E_{c.m.}$ (MeV)	l ($\hbar$)	λ_0 (sec^{-1})	$\log_{10}T_{1/2}$ (sec) Present	Ref. [13]	Experiment
1	^{221}Fr	(^{14}C)	29.28	3	0.579×10^{-5}	14.63	13.5	> 15.77
2	^{221}Ra	(^{14}C)	30.34	2	0.101×10^{-2}	12.39	11.7	> 14.35
3	^{222}Ra	(^{14}C)	30.87	0	0.306	10.91	10.6	11.02 ± 0.06
4	^{223}Ra	(^{14}C)	29.85	4	0.346×10^{-5}	15.85	13.2	15.2 ± 0.05
5	^{224}Ra	(^{14}C)	28.63	0	0.130×10^{-5}	16.27	16.3	15.9 ± 0.12
6	^{225}Ac	(^{14}C)	28.57	4	0.116×10^{-6}	17.33	17.7	> 18.34
7	^{226}Ra	(^{14}C)	26.46	0	0.159×10^{-10}	21.20	22.0	21.33 ± 0.2
8	^{231}Pa	(^{23}F)	46.68	0	0.108×10^{-8}	24.51		> 24.61
9	^{230}Th	(^{24}Ne)	51.75	0	0.390×10^{-10}	24.89	26.2	24.64 ± 0.07
10	^{232}Th	(^{26}Ne)	49.70	0	0.101×10^{-13}	29.07	31.7	> 27.94
11	^{231}Pa	(^{24}Ne)	54.14	0	0.103×10^{-7}	22.48	22.8	23.38 ± 0.08
12	^{232}U	(^{24}Ne)	55.86	0	0.112×10^{-5}	20.44	21.0	21.06 ± 0.1
13	^{233}U	(^{24}Ne)	54.27	0	0.106×10^{-10}	24.52	24.3	24.83 ± 0.15
14	^{233}U	(^{25}Ne)	54.32	0	0.765×10^{-8}	24.41		24.83 ± 0.15
15	^{234}U	(^{24}Ne)	52.81	0	0.705×10^{-11}	25.86	27.5	25.25 ± 0.05
16	^{234}U	(^{26}Ne)	52.87	0	0.211×10^{-10}	25.77	28.0	25.25 ± 0.05
17	^{234}U	(^{28}Mg)	65.26	0	0.785×10^{-10}	26.16	28.2	25.75 ± 0.06
18	^{237}Np	(^{30}Mg)	65.52	2	0.151×10^{-10}	27.19	29.1	> 27.27
19	^{238}Pu	(^{30}Mg)	67.00	0	0.603×10^{-10}	25.87	27.5	25.7 ± 0.15
20	^{238}Pu	(^{28}Mg)	67.32	0	0.793×10^{-10}	26.51	28.8	25.7 ± 0.25
21	^{238}Pu	(^{32}Si)	78.95	2	0.116×10^{-9}	26.02	28.6	25.3 ± 0.16
22	^{241}Am	(^{34}Si)	80.60	0	0.618×10^{-9}	25.75	26.4	> 25.3

one should not underestimate the uncertainties and limitations of the present approach.

Next, we report our results concerning the possibility of CR in the trans-tin region where the experimental activity is now concentrated [27,28]. The emissions energies in this region are calculated from actual nuclear masses [29] with the exception of the ^{114}Ba nucleus. For this we choose the extrapolated values of Ref. [30]: $Q_\alpha = 3.601$ MeV and $Q_{^{12}C} = 20.62$ MeV. The significant results for ^{16}O emission from ^{122}Ce, ^{114}Ba, ^{120}Ce, and ^{114}Cs nuclei and for ^{12}C emission from ^{114}Ba and ^{114}Cs nuclei are shown (in the order of increasing half-lives) on the right side of Fig. 3.

The shortest half-life in Fig. 3 ($T_{1/2} = 10^{5.43}$ s) corresponds to the ^{12}C emission from ^{114}Ba. Here we get a superallowed ^{12}C emission with an unexpected large branching ratio relative to alpha decay of $B = 10^{-3.7}$. We mention that this branching ratio was completely estimated in the present model by calculating the absolute rates of α and ^{12}C emissions (with expected errors within about one order of magnitude). This branching ratio is in good agreement with the rough experimental value of about $B \approx 10^{-4}$ [27]. Our half-life estimates in the trans-tin region are smaller by four orders magnitude than the first systematic predictions of Ref. [31] and agree with some predictions of Ref. [23].

In Fig. 3 we observe that the data for $\log_{10}T_{1/2}$ plotted vs $Q^{-1/2}$, where Q is the emission energy, roughly fall on a straight line for a series of different parent nuclei emitting the clusters with the charge numbers Z_c =6,8,10,12,14 (the dashed lines correspond to the charge number of the clusters). This trend is the same with the Geiger-Nuttall systematic trend well known for the alpha half-lives. However, energy constant B from the Geiger-Nuttall law ($\log_{10}T_{1/2}=BQ^{-1/2} + C$) seems to be the same for all CR, while the constant C seems to depend strongly on the structure of the emitted cluster.

We can see in Table I that the measured half-lives of CR leading to the magic-plus-two-neutrons fragments are larger in average by four orders of magnitude than half-lives of CR leading to the magic core $_{82}$Pb$_{126}$. Such differences that which suggest strong pairing correlations are well reproduced by the present model, as is expected. In general, large CR half-lives of actinide nuclei are evidently correlated with large neutron excess. On the other hand, with the increasing of neutron deficit in "exotic" trans-tin nuclei, a very strong proton-neutron interaction [32] comes into play due to the fact that the protons and neutrons occupy identical or energetically close-lying shell orbits. So, the neutron deficient trans-tin nuclei exhibit unusual properties such as new decay modes (proton, alpha, and cluster) [15,27,28], extremely large decay energies, very short half-lives, and now, new magic nucleon numbers far from stability.

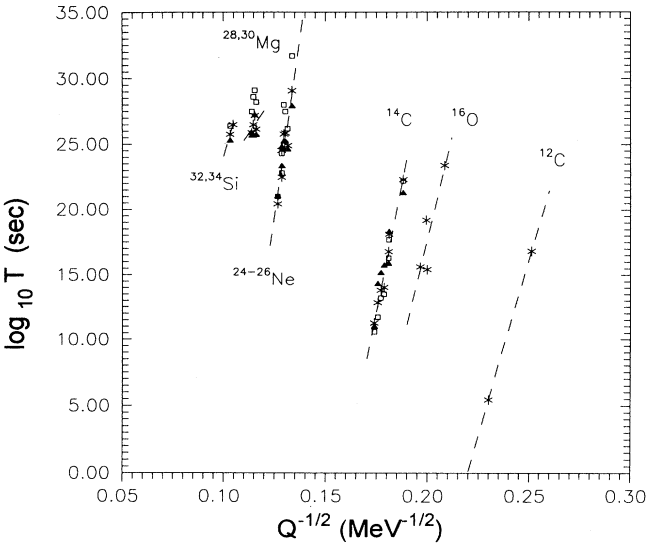

FIG. 3. Calculated and experimental half-lives of cluster radioactivities as a function of $Q^{-1/2}$ in a Geiger-Nuttall plot. The results of this work are shown by asterisks. The dashed lines, representing calculated cluster radioactivities, are drawn to guide the eye. The results of Ref. [13] are shown by open squares. The experimental data taken from the review of Ref. [22] are shown by full triangles.

VII. SUMMARY AND CONCLUSIONS

The main facts that a theory of CR must explain are (1) the empirical Geiger-Nuttall law; (2) a strong dependence of decay of decay rates on the periodicities in the nuclear structure, emission energies, and fragment interaction as a result of the clustering with valence nucleons; (3) "fine structure" effects related to the dissipation of the energy and angular momentum. These facts can be understood in terms of the semiclassical approximation for the penetration factor and the microscopical approximation of the clustering process. We present here an approach which accounts for all of these, and in addition gives a reasonable quantitative agreement with available decay rate data. Furthermore, we prove that the major contribution to the one-body width is given by the resonance amplitude of the Breit-Wigner type associated with the fragment scattering. This indicates that the scattering of two macroscopic superfluid objects may approximate the decay by emission of complex clusters.

The present calculations, based on a rather general and idealized model containing all the ingredients relevant for clustering and tunneling in the many particle nuclear system, give a good account of decay properties of nuclei. When the parameters of the theory are determined from the reaction cross section, we get an agreement with experimental decay rates within about one order of magnitude. This agreement, as well as the fact that we can describe the main features of natural decays, is clear evidence that our approach is essentially correct. The present approach contains, in very transparent form, all the basic elements for treatment of the interplay between the nuclear structure and reaction dynamics. The information on the clustering is contained in the CFA, which is deduced in the CHM approximation by using an harmonic-oscillator basis. The tunneling dynamics is treated in IF by solving numerically the motion equations containing the realistic potentials. These potentials are mainly deduced from scattering data at Coulomb energies. The relative wave functions relevant for the resonance tunneling are the resonance wave functions. In fact, we calculated the rates of the cluster production by the resonance decay, combining the CHM and IF. The width formula is presented in a final form that is independent of arbitrary channel radius parameter or surface terms (as a reduced width and penetrability), which depend on boundary conditions at this radius. This formula may be generalized to include more elaborated cluster shell model amplitudes [24–26].

Note particularly that the proposed numerical procedure requires a minimum of programming and makes use of the elementary codes for the nuclear structure and standard codes for the reaction dynamics. The computing time for the CHM cluster formation amplitude was substantially reduced in comparison with the usual shell model calculations.

We have shown that there is a very close connection between the CFA, the effective potential of the Schrödinger equation, and the node structure of the wave function of the relative motion of the fragments. Perhaps the most important conclusion of this study is that the clustering and resonance scattering phenomena in CR are very closely related to the occurrence of some specific very compact structures. Such structures frequently occur in other nuclear reactions [8], namely, in cold fission and different fusion processes. We estimated the probability of formation of these structures by solving a problem in which few nucleons interact via constant negative matrix elements in a small shell above the Fermi surface. In more accurate calculations one should take into account the anisotropy in the Fermi surface and redefine the matrix elements of pairing interaction in terms of microscopic quantities. The model can be improved by incorporating some features of the pairing dynamics.

The present study of CR in the lead and trans-tin regions allows one to gain new insights into nuclear structure and reaction mechanism aspects. In further investigations one should study in detail the mechanism of formation and decay of nuclear quasimolecules. It is to be expected that new accurate measurement of resonance properties of CR will give a precious information about the reaction mechanism.

We hope these results will provide some guidance in the study of cluster decay phenomena.

ACKNOWLEDGMENTS

We acknowledge with thanks the help and advice of our colleagues at the Institut für Theoretische Physik der Justus-Liebig-Universität Giessen and at the Institute for Atomic Physics Bucharest. I.S. acknowledges the hospitality of the Institut für Theoretische Physik der Justus-Liebig-Universität Giessen where this work was started. This work was carried out in the frame of the Scientific-Technical Romanian-German Collaboration and supported by BMFT (Bonn).

[1] A. Sandulescu, D.N. Poenaru, and W. Greiner, Sov. J. Part. Nucl. **11**, 528 (1980); D.N. Poenaru, M. Ivascu, A. Sandulescu, and W. Greiner, Phys. Rev. C **32**, 572 (1985).
[2] J.H. Rose and C.A. Jones, Nature **307**, 245 (1984).
[3] L. Brillard, A.G. Elayi, E. Hourani, M. Hussonnois, J.F. Le Du, L.H. Rosier, and L. Stab, C.R. Acad. Sci. Paris **309**, 1105 (1989); M. Hussonnois, J.F. Le Du, L. Brillard, J. Dalmasso, and G. Ardisson, Phys. Rev. C **43**, 2599 (1991).
[4] P.B. Price, K.J. Moody, E.K. Hulet, R. Bonetti, and C. Migliorino, Phys. Rev. C **43**, 1781 (1991).
[5] M. Greiner and W. Scheid, J. Phys. G **12**, L229 (1986).
[6] M. Ivascu and I. Silisteanu, Nucl. Phys. **A485**, 93 (1988); I. Silisteanu and M. Ivascu, J. Phys. G **15**, 1405 (1989).
[7] M. Ivascu and I Silisteanu, Sov. J. Part. Nucl. **21**, 589 (1990).
[8] A. Sandulescu and W. Greiner, Rep. Prog. Phys. **55**, 1423 (1992); A. Ludu, A. Sandulescu, and W. Greiner, Int. J. Mod. Phys. E **1**, 169 (1992).
[9] P. Arve, G.F. Bertsch, J.W. Negele, and G. Puddu, Phys. Rev. C **36**, 2018 (1987).
[10] F. Barranco, R.A. Broglia, and G.F. Bertsch, Phys. Rev. Lett. **60**, 507 (1988).
[11] V.G. Soloviev, Phys. Lett. **1**, 202 (1962); H.J. Mang and J. Rasmussen, Mater. Fys. Skr. Dan. Vid. Selsk. **2**(3), 1 (1962).
[12] J.P. Elliot, A.D. Jakson, H.A. Mavromatis, E.A. Sunderson, and B. Singh, Nucl. Phys. **A121**, 241 (1968).
[13] F. Barranco, G.F. Bertsch, R.A. Broglia, and E. Vigezzi, Nucl. Phys. **A512**, 235 (1990).
[14] G. Breit, in *Encyclopedia of Physics*, edited by S. Flugge (Springer, Berlin, 1959), Vol. 41, p. 34.
[15] H. Feshbach, Ann. Phys. (N.Y). **19**, 287 (1962).
[16] T. Matsuse, A. Arima, and S.M. Lee, Phys. Rev. C **26**, 2338 (1982).
[17] R.P. Cristiansen and W. Winter, Phys. Lett. B **65**, 27 (1977).
[18] A.R. Barnett and J.S. Lilley, Phys. Rev. C **9**, 2010 (1974).
[19] J.J. Kolata, K.E. Rehm, D.G. Kovar, G.S.F. Stephens, G. Rosner, H. Ikezoe, and G. Wojtech, Phys. Rev. C **30**, 125 (1984).
[20] E.E. Gross, T.D. Clearby, I.L.C. Ford, Jr., D.C. Hensley, K.S. Toth, F.T. Baker, A. Scott, C.R. Bringham, and T.A. Vrba, Phys. Rev. C **29**, 449 (1984).
[21] H. Friedrich and K. Langanke, Phys. Rev. C **28**, 1385 (1983).
[22] P.B. Price, Annu. Rev. Nucl. Part. Sci. **39**, 147 (1989), and references therein.
[23] S. Kumar and R.K. Gupta, Phys. Rev. C **49**, 1922 (1994); R.K. Gupta, S. Singh, R.K. Puri, A. Sandulescu, W. Greiner, and W. Scheid, J. Phys. G **18**, 1533 (1992).
[24] R. Blendovske, T. Fliessbach, and H. Walliser, Z. Phys. A **339**, 121 (1991).
[25] A. Sandulescu, I. Silisteanu, and R. Wünsch, Nucl. Phys. **A305**, 205 (1978).
[26] A. Insolia, P. Curutchet, R.J. Liotta, and D.S. Delion, Phys. Rev. C **44**, 545 (1991); K. Varga, R.G. Lovas, and R.J. Liotta, Nucl. Phys. **A550**, 421 (1992); D.S. Delion, A. Insolia, and R.J. Liotta, J. Phys. G **19**, L189 (1993).
[27] S.P. Tretyakova, I.N. Micheev, and Yu. Ts. Oganessian (private comunication).
[28] H. Roeckl and O. Klepper (private communication); (unpublished).
[29] G. Audi and A.H. Wapstra, Nucl. Phys. **A565**, 1 (1993).
[30] W. Scheid, I. Silisteanu, and A. Sandulescu, Rom. J. Phys. **38**, 331 (1993); I. Silisteanu, W. Scheid, and M. Ivascu, *ibid.* **38**, 329 (1993).
[31] W. Greiner, M. Ivascu, D.N. Poenaru, and A. Sandulescu, in *Treatise on Heavy-Ion Science*, edited by D. Allen Bromley (Plenum, New York, 1988), Vol. 8; D.N. Poenaru, W. Greiner, and R. Gherghescu, Phys. Rev. C **47**, 2030 (1993).
[32] W. Scheid and I. Silisteanu (unpublished); G. Popa, A. Sandulescu, I. Silisteanu, and W. Scheid, in *Frontiers Topics in Nuclear Physics*, NATO ASI Series B: Physics, edited by W. Scheid and A. Sandulescu (Plenum, New York, 1994), p. 71.